Equal channel spacing Sagnac filter using high-birefringent photonic crystal fibers

Xiurong Ma (马秀荣)[1,2*] and Ying Zhu (朱 颖)[1,2]

[1] *School of Computer and Communication Engineering, Tianjin University of Technology, Engineering Research Center of Communication Devices, Ministry of Education, Tianjin 300384, China*

[2] *Tianjin Key Laboratory of Film Electronic and Communication Device, Tianjin 300384, China*

[*] *E-mail: swency@163.com*

Received March 1, 2010

An equal channel spacing Sagnac filter is proposed using a high-birefringent photonic crystal fiber (PCF) with birefringence square to the operation wavelength. A PCF with four smaller central air holes surrounded by larger air holes is applied in a Sagnac filter with optimized parameters to achieve equal channel spacing of 0.8 nm. Given that the birefringence of this PCF is square to the operation wavelength, the channel spacing of the proposed filter changes by only 0.03 nm within a wavelength range from 1400 to 1650 nm; this is about one order of magnitude less than that constructed with conventional high-birefringent fibers.

OCIS codes: 060.2330, 060.2340, 060.2420, 230.7408.

doi: 10.3788/COL20100810.0983.

Currently, the popularity of the dense wavelength-division multiplexing (DWDM) system in long-haul optical communications has attracted great interest in the field of DWDM filters. As one of the most important filters in these systems, Sagnac filters[1,2] are especially valued because they could realize a higher extinction ratio, a narrower filter bandwidth, an independence of input polarization, a lower susceptibility to environmental noises[3−5], etc. Channel spacing of DWDM filters applied in optical communication systems should fulfill the requirement recommended by the ITU-T (i.e., 0.8 nm). Variations in channel spacing will lead to a series of adverse effects in the DWDM system, such as channel shift and channel interference[6,7]. However, channel spacing of conventional Sagnac filters changes with operation wavelength, which should be given sufficient consideration.

In this letter, an equal channel spacing Sagnac filter is proposed using a high-birefringent photonic crystal fiber (Hi-Bi PCF)[8−12] with birefringence square to operation wavelength. We apply this method to create a Sagnac filter based on a PCF with four smaller central air holes. The channel spacing changes by only 0.03 nm within the wavelength range from 1400 to 1650 nm; this is about one order of magnitude smaller than that of the Sagnac filters constructed with conventional high birefringent fibers (HBFs).

Figure 1 shows the structure of a conventional Sagnac filter. The filter is composed of a 3-dB coupler, a polarization controller (PC), a section of HBF depicted by the thick line inside the loop, and two sections of normal single-mode fibers used to connect the HBF with the coupler. The input light was split into two counter-propagating beams by the 3-dB coupler. The two beams recombined and interfered at the coupler after propagating through the whole fiber loop. From this, a DWDM light consisting of different wavelengths was obtained from the output port in accordance with their interference states determined by the phase difference between the two orthogonally-polarized elements of the fundamental mode traveling in the loop. The polarization controller (PC) was used to adjust the angle between the input light and the fast axis of a PCF.

The channel spacing of the Sagnac filter can be given as[13]

$$\Delta\lambda(\lambda) = \frac{\lambda^2}{B(\lambda)L}, \tag{1}$$

where $\Delta\lambda(\lambda)$ is the channel spacing, λ is the operation wavelength, $B(\lambda)$ is the birefringence, and L is the length of the birefringent fiber. As a function of the wavelength, $B(\lambda)$ is given as[14]

$$B(\lambda) = \frac{\lambda}{L_{\mathrm{B}}}, \tag{2}$$

where L_{B} is the polarization beat length of the birefringent fiber.

Combining Eqs. (1) and (2), we can obtain

$$\Delta\lambda = \frac{\lambda L_{\mathrm{B}}}{L}. \tag{3}$$

From Eq. (1), it is apparent that the channel spacing of a conventional Sagnac filter varies with the operation wavelength. Thus, if the birefringence is square to the operation wavelength, then the channel spacing of the Sagnac filter would become equal. Considering a smart construction, it is possible to achieve a kind of PCF with the above characterization. This PCF birefringence can be expressed as

$$B(\lambda) = \alpha\lambda^2, \tag{4}$$

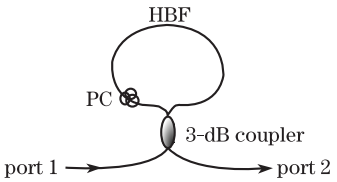

Fig. 1. Structure of a conventional Sagnac filter.

where α is a constant. Substituting Eq. (1) with Eq. (4), we can obtain

$$\Delta\lambda = \frac{1}{\alpha L}. \tag{5}$$

From it, we can see that the channel spacing of the PCF Sagnac filter remains constant.

To construct a Sagnac filter with equal channel spacing, we designed a Hi-Bi PCF with four smaller central air holes and calculated the birefringence as a function of wavelength. The cross section of the proposed index-guiding PCF is shown in Fig. 2(a). Here, four smaller air holes near the core were introduced into the cladding, replacing the corresponding larger air holes. The air holes were arranged in a triangular lattice of pitch Λ. The PCF was characterized by the hole pitch along x- and y-directions (i.e., Λ_x and Λ_y), small air hole diameter d_1, and large air hole diameter d_2.

The refractive index of fused silica was assumed to be 1.45 and the refractive index of the air holes was set as 1 in our simulation. The geometric symmetry of the proposed PCF allowed just one-quarter of the structure to be considered in an efficient simulation (Fig. 2(b)).

To calculate the propagation constants of the fundamental modes, we used a full-vector finite-element method[15]. The birefringence can be expressed as

$$B(\lambda) = \frac{\lambda}{2\pi}[\beta_y(\lambda) - \beta_x(\lambda)], \tag{6}$$

where λ is the operation wavelength of light, β_x and β_y are the respective propagation constants of the two orthogonal polarization modes.

For the proposed PCF, given that the value of birefringence is relevant to the structure parameters of the PCF, we first considered the effect on birefringence by designing the size of small air holes. Figure 3 shows the relationship between the birefringence and the operation wavelength of the proposed PCF with different small air diameters d_1, where $d_2 = 0.6\Lambda$ and $\Lambda = 1.96$ μm. All of the four birefringence curves increase monotonically as wavelength increases; in addition, the value of the birefringence increases with decreasing d_1. We fitted these curves using quadratic polynomial $B(\lambda) = A_0 + A_1 \times \lambda + A_2 \times \lambda^2$. The fitting coefficients A_0, A_1, and A_2 are listed in Table 1. From Table 1, we can see that $|A_2| - |A_1|$ increases as d_1 decreases. Therefore, $d_1 = 0.2\Lambda$ and $d_2 = 0.6\Lambda$ were selected in our simulation.

Table 1. Fitting Coefficients with Different d_1

d_1/Λ	A_0	A_1	A_2	$\lvert A_2\rvert - \lvert A_1\rvert$
0.2	4.6712×10^{-5}	–446.11801	9.50932×10^{8}	9.50932×10^{8}
0.3	1.07046×10^{-4}	–532.92484	8.7268×10^{8}	8.72679×10^{8}
0.4	1.12723×10^{-4}	–559.56611	6.70166×10^{8}	6.70165×10^{8}
0.5	6.95433×10^{-4}	–568.00012	3.75476×10^{8}	3.75475×10^{8}

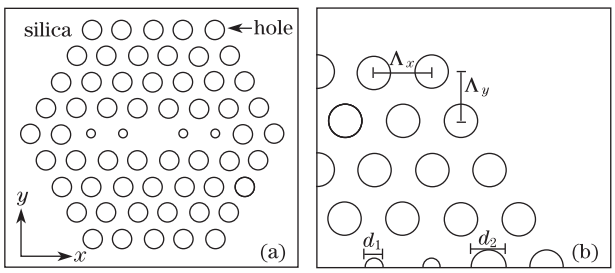

Fig. 2. (a) Cross section of the birefringent PCF and (b) one quarter of the fiber cross section.

Next, we considered how changing the size of the large air holes could affect birefringence. Figure 4 shows the birefringence of the proposed PCF with different large air hole diameters d_2, where $d_1 = 0.2\Lambda$ and $\Lambda = 1.96$ μm. From Fig. 4, we can see that the value of birefringence increases as d_2 increases. We also fitted these curves using the quadratic polynomial $B(\lambda) = A_0 + A_1 \times \lambda + A_2 \times \lambda^2$. The fitting coefficients A_0, A_1, and A_2 are listed in Table 2.

The effects of the hole pitch Λ on the birefringence values of the PCF when $d_1 = 0.2\Lambda$ and $d_2 = 0.6\Lambda$ were examined. The results are presented in Fig. 5. We can find that the birefringence value increases as Λ decreases. We also fitted these curves using quadratic polynomial $B(\lambda) = A_0 + A_1 \times \lambda + A_2 \times \lambda^2$. The fitting coefficients A_0, A_1, and A_2 are listed in Table 3. From it, we can see that $|A^2| - |A^1|$ increases as Λ decreases. In addition, when $\Lambda = 1.72$ μm, A_2 became higher than A_0 and A_1 by at least a seven-order magnitude. Therefore, A_0 and

Table 2. Fitting Coefficients with Different d_2

d_2/Λ	A_0	A_1	A_2	$\lvert A_2\rvert - \lvert A_1\rvert$
0.3	-8.41248×10^{-5}	168.43027	-2.58611×10^{7}	2.58609×10^{7}
0.4	-1.15961×10^{-4}	163.13483	1.23867×10^{8}	1.23867×10^{8}
0.5	-6.65265×10^{-5}	–255.19433	4.53939×10^{8}	4.53939×10^{8}
0.6	4.6712×10^{-5}	–446.11801	9.50932×10^{8}	9.50932×10^{8}

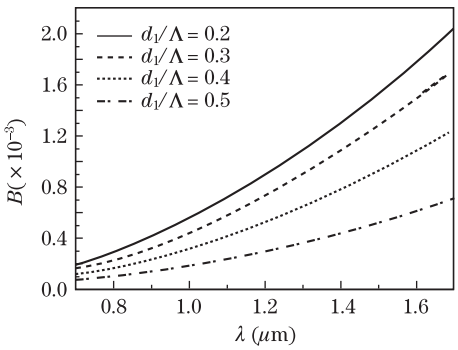

Fig. 3. Birefringence as a function of wavelength from 700 to 1700 nm with different d_1.

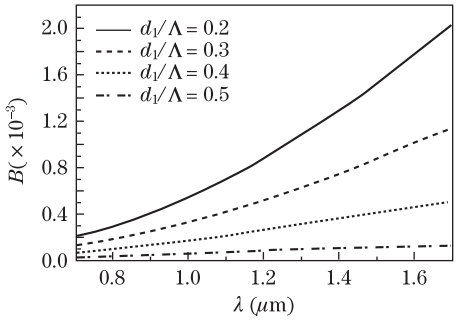

Fig. 4. Birefringence as a function of wavelength from 700 to 1700 nm with different d_2.

Table 3. Fitting Coefficients with Different Λ

Λ(μm)	A_0	A_1	A_2	$\lvert A_2\rvert - \lvert A_1\rvert$
1.72	-1.41191×10^{-4}	−127.03416	1.05621×10^{9}	1.05621×10^{9}
1.96	4.6712×10^{-5}	−446.11801	9.50932×10^{8}	9.50932×10^{8}
2.2	1.19827×10^{-4}	−529.39723	8.11039×10^{8}	8.11038×10^{8}

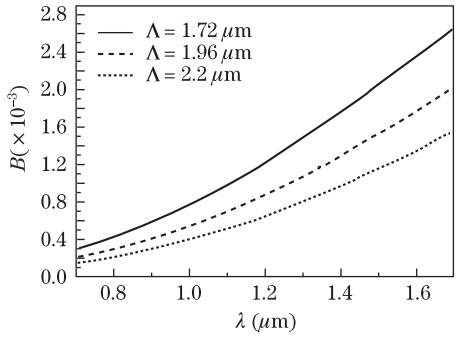

Fig. 5. Birefringence as a function of wavelength from 700 to 1700 nm with different Λ.

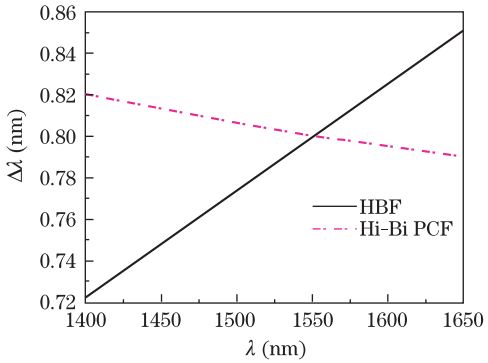

Fig. 6. Channel spacing as a function of operation wavelength from 1400 to 1650 nm.

A_1 could be neglected in the following simulation.

According to the above explanation, by setting the structure parameters $\Lambda = 1.72$ μm, $d_1 = 0.2\Lambda$, and $d_2 = 0.6\Lambda$ of the Hi-Bi PCF, $B(\lambda)$ can be expressed in the following formula under quadratic polynomial fitting:

$$B(\lambda) = -1.41191\times10^{-4} - 127.03416\lambda + 1.05621\times10^{9}\lambda^2. \quad (7)$$

From the above, the respective channel spacing of Hi-Bi PCF- and conventional HBF-based Sagnac filters (polarization beat length $L_B = 2.45$ mm) within a certain wavelength range can be calculated. If the channel spacing of the two Sagnac filters remains 0.8 nm at 1550 nm, the lengths of the PCF and the conventional HBF filters could be calculated according to Eqs. (1), (2), and (3), respectively. The length of ordinary HBF is $L \approx 4.75$ m, and that of the proposed PCF is $L' \approx 1.364$ m.

From the above results, we can obtain the respective variation curves of the channel spacing of Sagnac filter based on ordinary HBF and PCF as the operation wavelength changes. Figure 6 illustrates the variations in channel spacing as a function of operation wavelength from 1400 to 1650 nm for two different fibers of the Sagnac filters. It is apparent that the channel spacing of the proposed Sagnac filter changes by only 0.03 nm, and is one order of magnitude smaller than that of the Sagnac filter constructedly using the conventional HBF. This indicates that the proposed Sagnac filter has approximately equal channel spacing.

In conclusion, we demonstrate the design of a Sagnac filter with equal channel spacing. As an example, we design a Hi-Bi PCF with a birefringence square to operation wavelength. A Sagnac filter with channel spacing which changes by only 0.03 nm from 1400 to 1650 nm is achieved; this is about one order of magnitude smaller than that of Sagnac filters constructed with conventional HBF.

This work was supported by the Key Project of the Ministry of Education (No. 206006), the Tianjin Key Project of Applied and Basic Research Programs (No. 07JCZDJC06000), and the Tianjin Project of the Committee of Education (No. 2006BA30).

References

1. Y. Han, Q. Li, X. Liu, and B. Zhou, IEEE Photon. Technol. Lett. **11,** 90 (1999).
2. X. P. Dong, S. Li, K. S. Chiang, M. N. Ng, and B. C. B. Chu, Electron. Lett. **36,** 1609 (2000).
3. C.-L. Zhao, X. Yang, C. Lu, W. Jin, and M. S. Demokan, IEEE Photon. Technol. Lett. **16,** 2535 (2004).
4. X. Ma, Z. Wu, and Y. Liu, G. Kai, S. Yuan, X. Dong. J. Optoelectron. Laser. (in Chinese) **15,** 885 (2004).
5. H. C. Lim, F. Futami, and K. Kikuchi, IEEE Photon. Technol. Lett. **11,** 578 (1999).
6. J. L. Jackel, J. E. Baran, G.-K. Chang, M. Z. Iqbal, G. H. Song, W. J. Tomlinson, D. Fritz, and R. Ade, IEEE Photon. Technol. Lett. **7,** 370 (1995).
7. T. Ohtsuki, IEEE Photon. Technol. Lett. **16,** 520 (1998).
8. Y. Yue, G. Kai, Z. Wang, Y. Lu, C. Zhang, T. Sun, Y. Li, L. Jin, J. Liu, Y. Liu, S. Yuan, and X. Dong, IEEE Photon. Technol. Lett. **18,** 2638 (2006).
9. Y. Yue, G. Kai, Z. Wang, T. Sun, L. Jin, Y. Lu, C. Zhang, J. Liu, Y. Li, Y. G. Liu, S. Yuan, and X. Dong, Opt. Lett. **32,** 469 (2007).
10. P. R. Chaudhuri, V. Paulose, C. Zhao, and C. Lu, IEEE Photon. Technol. Lett. **16,** 1501 (2004).
11. X. Zhang, J. Zhao, and L. Cui,. Acta Opt. Sin. (in Chinese) **28,** 1379 (2008).
12. T. Gong, F. Yan, L. Wang, Y. Li, P. Liu, and S. Jian, Chinese J. Lasers (in Chinese) **35,** 559 (2008).
13. S. Yang, Z. Li, X. Dong, S. Yuan, G. Kai, and Q. Zhao, IEEE Photon. Technol. Lett. **14,** 774 (2002).
14. W. Sun, F. Fu, X. Liu, Y. Jiang, and J. Zhang, Chinese J. Lasers (in Chinese) **36,** 884 (2009).
15. F. Zhang, X. Liu, M. Zhang, and P. Ye, Acta Photon. Sin. (in Chinese) **36,** 209 (2007).